International Journal of Air-Conditioning and Refrigeration Vol. 15, No. 4 (2007) 147~155

A Dynamic Test Facility for Mobile Air Conditioning Systems

Amr Gado, Yunho Hwang*, Reinhard Radermacher

Center for Environmental Energy Engineering, University of Maryland, College Park, Maryland, USA

(Received September, 10, 2007; Revision received November 11, 2007)

Abstract

Mobile air conditioning systems work under widely changing operating conditions. To understand the system behavior under such dynamic conditions, a test facility that can impose transient loads as well as conducting dynamic measurements is needed. To test mobile air conditioning systems including their dynamic performance under various drive cycle patterns without using full scale vehicles in a wind tunnel, a new test facility, called "dynamic simulator," is described. It can replicate real vehicle operating conditions by interacting with the system being tested based on the measured system performance and subsequently adjusting the air properties returning to the test system based on the results of a numerical cabin model. A new dynamic simulator has been designed, constructed, and verified for performing dynamic tests. It was successful in controlling the temperature and relative humidity of the air returning to the test unit within ± 0.7°C and ± 4% of their respective intended values. The verification test under the New European Driving Cycle demonstrated that detailed transient behavior of the mobile air conditioning system could be measured by using this dynamic simulator.

Key words: Dynamic; Simulator; Mobile; Air conditioning system; Cabin model

Nomenclature

a	: Anticipation factor, dimensionless
A/I	: Analog Input
AHU	: Air Handling Unit
A/O	: Analog Output
Cp	: Specific heat at constant pressure, kJ/kg-K
C	: Specific heat, kJ/kg-K
D	: Derivative constant
D/I	: Digital Input
D/O	: Digital Output
e	: Error, difference between set point and process value for a controlled parameter.
e'	: Error of the next step, difference between set point of the next control step and process value of a controlled parameter, if known.
f	: Function
h	: Enthalpy, kJ/kg
I	: Integral constant
M	: Mass, kg
MAC	: Mobile Air Conditioning
NEDC	: New European Drive Cycle
P	: Proportional constant
PID	: Proportional-Integral-Derivative
Q	: Load or capacity, kW
RH	: Relative Humidity, %
RPM	: Revolution Per Minute
S	: Set point of any controlled parameter
T	: Temperature, K
t	: Time, s
W	: Humidity ratio, kg/kg

Subscript:

Amb	: Ambient air
adj	: Adjusted
c	: Core, or interior mass
e	: Evaporator
fg	: Latent heat
m	: Mixture, or return air
ps	: Passengers, sensible
pl	: Passengers, latent
r	: Room, or inside of cabin
s	: Supply air
sol	: Solar radiation

*Corresponding author. Tel.: +1-301-405-5247, Fax.: +1-301-405-2025
E-mail address: yhhwang@eng.umd.edu

1. Introduction

Mobile air conditioning systems, termed here MAC, provide not only safe driving conditions by securing fair visibility and also driver's alertness by maintaining thermal comfort conditions under severe weather conditions. They are exposed to various operating conditions that are determined by thermal loads, exterior weather conditions, and driving patterns. Among these parameters, driving patterns directly affect the rotational speed of the compressor and the outdoor coil face velocity, and have a major impact on the performance of the MAC. These variations in parameters affect the operation of the MAC, such as operating pressure levels, degrees of subcooling and superheating, refrigerant quality entering the evaporator, refrigerant mass flow rate, and refrigerant charge distribution along the cycle components. Due to difficulties in imposing dynamic thermal loads to the MAC, three approaches to test the MAC during its transient operation have been implemented. The first method, which is the most popular, is testing of the MAC by using a full scale vehicle in the wind tunnel large enough to house the vehicle [1, 2]. The second is numerical modeling [3-8]. The third is placing a hot water heat exchanger in the same duct where the test evaporator is installed to impose some thermal storage effect to simulate pulldown conditions [9, 10]. These three methods have some disadvantages such as either requiring a large and costly facility or not being able to provide a realistic load profile on the evaporator as it may occur during a drive cycle. To capture the dynamic behavior of the MAC, a test facility should be able to: (a) run weather cycles to simulate change in outdoor air conditions, (b) run drive cycles to simulate the varying rotational speed of an automotive compressor and varying air velocities across the condenser, (c) simulate the thermal storage load of the conditioned space, (d) simulate changes in space loads resulting from a change in number of occupants and controls settings, (e) control the percentage of fresh air mixed with the supply air, (f) control the evaporator fan speed to simulate different user settings, (g) measure fast enough the properties of the refrigerant and the air, and the temperature of the metal of the system itself, and finally (h) to provide instantaneous values for latent and sensible capacities and compressor power. The goal of the current research is satisfying these requirements in a laboratory environment to provide economic means for conducting transient tests on MAC under realistic dynamic conditions. By conducting laboratory experiments on the MAC, important performance indicators, such as the sensible capacity and latent capacity, can be readily measured, which is difficult in the field tests

2. Dynamic simulator

To measure the dynamic performance of the MAC, a new approach using a typical environmental test facility, called "dynamic simulator," is proposed. The dynamic simulator measures the supply-air temperature and relative humidity of the air downstream of the evaporator coil, calculates the conditions of the return-air leaving the cabin returning to the evaporator coil using a numerical cabin model, and controls the air handling unit (AHU) of the indoor loop such that the air temperature and relative humidity are dynamically adjusted according to the return-air conditions calculated from the cabin model.

2.1 Review of previous cabin models

Ding and Zito [11] presented a first order differential equation that relates the cabin heat transfer coefficient, panel discharge temperature and volumetric air flow to average cabin air temperature. They suggested a method to experimentally determine overall heat transfer coefficient of the cabin but their model neglected thermal storage and latent loads as well as infiltration and passengers' loads. Other researchers; Choquart et al. [12], Huang and Han [13], Han et al. [14], and Aroussi and Aghil [15]; used CFD models to predict the cabin air conditions and obtained good agreement between their results and experimental results. CFD models require detailed dimensions of the cabin and the locations of the air vents and can produce detailed results of the spatial variation of the velocity and temperature fields inside the cabin and therefore are more suitable for assessing the thermal comfort of passengers or evaluating defrost conditions.

Huang (1998) developed a mathematical model that predicts the lumped temperature and humidity variations inside the cabin under design and operating conditions. The model is composed of four coupled nonlinear ordinary differential equations; namely, dry-air mass balance, moisture mass balance, cabin-air energy balance, and interior-mass energy balance.

However, the model uses a constant built-in ventilation rate and does not allow the change of supply airflow rate. Moreover, this model requires detailed information about the construction of the cabin, its color, characteristics of the glass, location of car, ground solar reflection coefficient, as well as height and weight of passengers.

Khamsi and Petitjean [16] modeled both the cabin and the A/C system components. Their model is based on a modular concept in which the elementary models of each component are coupled with the models of the other components. Very little is described in their work about the equations they used to model the cabin and the method of solution. Similar deficiencies exist in the works by Thelon and Zoz [17] and Kohler et al. [18]. Kataoka [19] used Navier-Stockes equation and the energy equation to predict the air velocity and temperature distribution in the cabin. He employed finite elements method based on the Cartesian coordinate system in spatial integration where a first order upwind scheme is applied to convection terms. For this, he divided the whole region into small cubic elements and therefore required very detailed geometric inputs.

Roy et al. [20] studied the thermal heat transfer in a car cabin and its effect on the equivalent temperature of the cabin and concluded that the radiative heat transfer is the most significant source responsible for energy consumption and passengers' discomfort. Their study employed in-house software. Several other commercial packages are available, such as KULI (Magna – Steyr [21]) and MACSim (ARMINES [22]), but these packages include closed-source software that can't be adapted to the present purpose.

2.2 The cabin model

From the foregoing literature review [11-22], it is apparent that most of previous cabin models require either significant computational time or are in closed source codes so that no model can readily serve the present purpose. Therefore, a new simplified model that requires only short computational time was developed. The assumptions of the cabin model used in this study are as follows:

- Solar load is constant.
- Radiation from cabin components to air is neglected.
- Latent and sensible loads of each passenger are constant.
- Heat transfer from engine compartment, trunk, and floor are neglected. This is due to the thermal insulation between these spaces and the cabin, as well as the lack of forced convection between them.
- Thermal storage in cabin walls is neglected for simplicity.
- Overall heat transfer coefficient of the cabin wall does not change with vehicle speed [23]. This is because the most significant component of the overall heat transfer is the internal convection.
- Heat transfer along air ducts is neglected.
- Properties of air and of interior mass are spatially uniform (lumped capacitance method) as used by several researchers [11, 24-26].
- The constituents of the interior mass have the same specific heat and temperature.

Eqs. 1 through 5 are used in the cabin model. For simplicity, the cabin sensible and latent loads are treated separately. However, the air properties are calculated at the corresponding temperature and humidity ratio in each time step. The sensible load portion of the cabin capacity is presented by Eqs. 1 through 3, which represent the energy balance of cabin air sensible heat, energy balance of interior mass and adiabatic mixing of dry air, respectively.

$$\begin{aligned} & M_r Cp_r \frac{dT_r}{dt} + M_c C_c \frac{dT_c}{dt} \\ &= -m_e Cp_e (T_m - T_s) + Q_{sol} + Q_{ps} + \\ & \quad U_o A_o (T_{amb} - T_r) + m_{iv} Cp_{amb} (T_{amb} - T_r) \end{aligned} \tag{1}$$

$$M_c C_c \frac{dT_c}{dt} = -h_c A_c (T_c - T_r) \tag{2}$$

$$\begin{aligned} & m_{iv} Cp_{amb} T_{amb} + (m_e - m_{iv}) Cp_r T_r \\ &= m_e Cp_m T_m \end{aligned} \tag{3}$$

The latent portion is presented by Eqs. 4 and 5, which represent the cabin air latent energy balance, and moisture mass balance at the mixing point before the coil, respectively.

$$\begin{aligned} M_r h_{fg} \frac{dW_r}{dt} = & - m_e h_{fg} (W_m - W_s) + \\ & m_{iv} h_{fg} (W_{amb} - W_r) + Q_{pl} \end{aligned} \tag{4}$$

Table 1. Input variables for cabin model

No.	Parameter	Value	Source
1	Ambient temperature and relative humidity	43.3°C and 65%	[24]
2	Solar load	950 W	[24]
3	Degree of soaking	16.7°C	[24]
4	Surface area of cabin	30 m^2	[24]
5	Overall heat transfer coefficient of cabin wall	4 W/m^2-K	[23]
6	Internal volume of cabin	8 m^3	[24]
7	Interior mass of cabin	200 kg	[24]
8	Specific heat of interior mass	400 J/kg-K	[24]
9	Surface area of interior mass	3 m^2	Typical value
10	Convective heat transfer coefficient between interior mass and cabin air	100 W/m^2-K	Estimated
11	Number of passengers	0	[24]
12	Amount of fresh air	0	[24]
13	Blower setting	120 g/s	Typical value
14	Supply air temperature	Profile	[24]
15	Supply air relative humidity	Profile	Typical profile

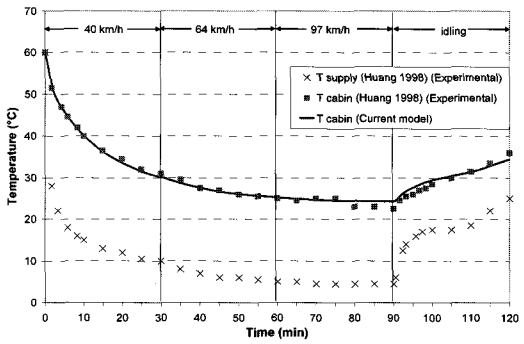

Fig. 1. Cabin model verification results.

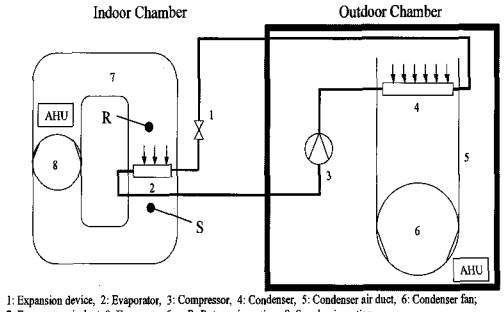

Fig. 2. Typical laboratory test facility for steady state testing.

$$(m_e - m_{iv})W_r + m_{iv}W_{amb} = m_e W_m \quad (5)$$

To verify the model pull-down experimental data of the MAC provided by Huang [24] was used. The overall (total) heat transfer coefficient of the cabin wall was chosen to be 4 W/m^2K [23]. Table 1 lists input variables needed for the current cabin models, and shows values used for the verification calculation. Figure 1 shows a comparison between the cabin air temperature from the model and the experimental results. An average deviation was 0.7°C, and a standard deviation was 0.6°C.

2.3 Dynamic control of test facility

To construct the dynamic simulator, some modifications were made to the AHU controllers of the typical steady state test facility, which is shown in Figure 2. Both the indoor and outdoor simulators control the temperature and relative humidity of supply air to test units by using AHUs with Proportional-Integral-Derivative (PID) controllers. The temperature controller actuates the hot-gas bypass valve, liquid-line valve, and the electric heater. The indoor loop fan, condenser duct fan and compressor motor are powered by means of variable frequency inverters. The temperature and humidity PID controllers and frequency inverters all accept remote set points in the form of an analog signal that the controller uses to scale the value of temperature, relative humidity (RH), or frequency, between specified upper and lower limits. There are two layers of control implemented on the dynamic simulator; viz. software control and hardware control. This concept is illustrated in Figure 3. The hardware control refers to the physical controllers that were part of the original test facility, while the software control refers to the control capability

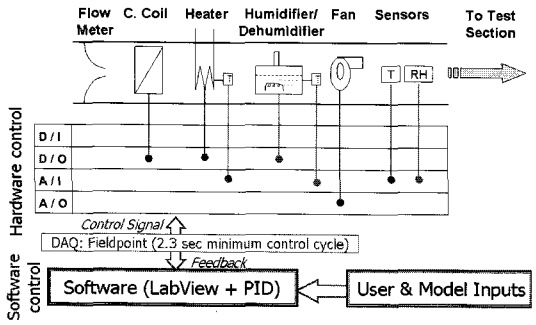

Fig. 3. Schematic of two control layers.

added through newly developed software.

The cabin model program sends remote set points to the temperature and humidity controllers to control the indoor loop temperature and RH. To enhance the accuracy of the control the PID control capability is added to cabin model program. Each time step, the program measures the process value of the controlled parameter upstream of the evaporator coil and calculates the error, e, which is the difference between the measured and the desired values. This error is used in a typical PID function shown in Eq. 6 to calculate the set point S_{adj}, where S denotes the controlled parameter, either temperature or RH.

$$S_{adj} = S + f_{PID}(e) = S + P.e + \frac{1}{I}\int e.dt + D\frac{de}{dt} \quad (6)$$

Therefore, the value of the set point that the program sends to the temperature or RH controller is not exactly the desired value which is the output of the cabin model, but an adjusted value based on the error. The P, I, and D factors were empirically tuned to yield the least error. When it is required to run a time-sequence of compressor RPM and condenser fan motor RPM that represents a drive cycle, or a time-sequence of outdoor temperature and RH that represents changes in weather conditions, the full time-sequence is known beforehand. The dynamic control software reads such information from the user input and executes the program. At each time step, the software measures the value of the controlled parameters and compares it with the desired values based on the simulation. The difference between the two values is the error, e, which the software uses to calculate the adjusted set point that is sent to the corresponding controller. In this case, the next set point is already known in each time step, therefore the dynamic control software takes advantage of this feature while sending the set points to the controllers by further adjusting the set points according to Eq. 7.

$$S_{adj} = S + f_{PID}\{(1-a)e + ae^{n}\} \quad (7)$$

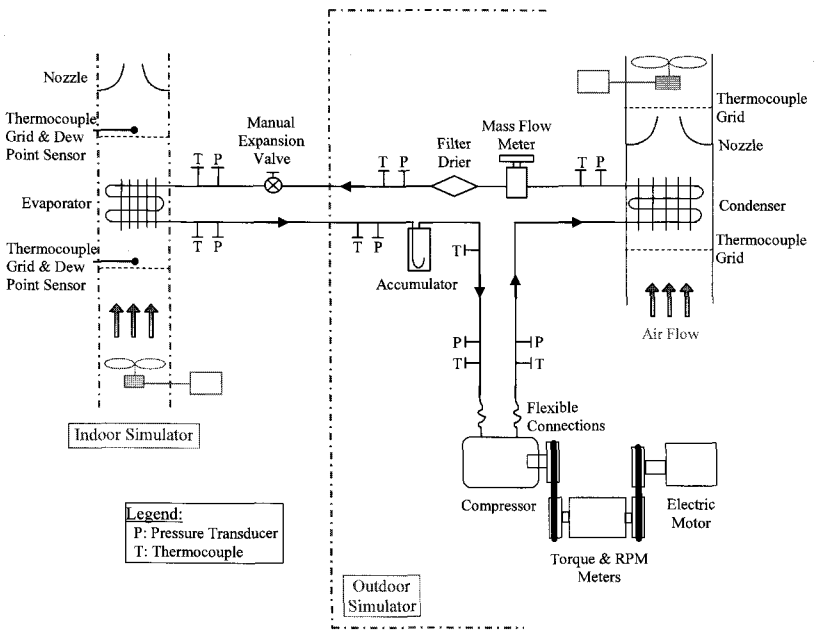

Fig. 4. Schematic diagram of the test system.

3. The experimental test system and instrumentation

A typical R134a mobile air conditioning system was constructed inside the chambers of the dynamic simulator. Figure 4 shows details of the test system. The system has a serpentine evaporator, a fin-and-tube condenser, a fixed area orifice, a suction accumulator, and an open-drive compressor. The open-drive compressor was driven by means of a 7.5 kW electric motor, which was operated by a variable frequency inverter.

Several thermocouples and pressure transducers were installed along the refrigerant circuit as indicated by the "T" and "P" symbols in Figure 4. A torque meter was mounted between the compressor and the electric motor. Also the rotational speed of the compressor was measured by means of an RPM sensor. A Coriolis mass flow meter was placed in the liquid line to measure the mass flow rate of refrigerant. All the thermocouples used were in-stream thermocouples having exposed junctions and 1.6 mm in diameter to minimize the response time. Grids of nine equally spaced thermocouples were used to measure the average air dry-bulb temperatures upstream and downstream of the coils. To calculate the latent capacity of the system dew point sensors before and after the evaporator were placed. It should be noted that the dew point sensors have the slowest time constant among instruments used although the fastest feasible one commercially available was used.

The volume flow rates of evaporator and condenser airs are measured by means of nozzles. All instruments were calibrated and the saturation temperature and pressure values were checked against each other to check the accuracy of measurements. Moreover, after each test, the capacities as calculated from the air side and from the refrigerant side were checked and the error was kept below 4%.

4. Verification of dynamic simulator

Two types of tests were conducted to verify the interaction between the dynamic simulator and the MAC being tested. In the first category, the unloaded test, which means operating only AHUs of the test facility but not the test system, parameters such as temperature, RH, air flow rate, and compressor RPM were controlled according to a pre-set profile to check the accuracy of dynamic simulator control. Figure 5 shows an example of this category of tests. It is clear that the error in controlling temperature was within ± 0.5°C and the error in controlling RH was within ± 2%. In the second category, the New European Drive Cycle (NEDC) [27] was imposed on the system according to the test conditions shown in Table 2 and Figure 6. The MAC was started in the beginning of the test. Figure 7 shows how air conditioning system parameters and performance are affected by the fluctuations of compressor speed based on the NEDC drive cycle. Figure 7-(a) shows the air temperature profiles inside the cabin, as calculated by the cabin model, and as measured inside the indoor simulator loop. The difference between these two values was less than 0.7°C, which shows how accurately the dynamic simulator controlled the temperature during the test. Figure 7-(b) shows the supply air and cabin air RHs as well as air mass flow rate. The difference between two RHs was less than 4% RH. It is clear that the supply air RH fluctuates as a result of the fluctuations in compressor RPM. The compressor rotational speed fluctuations affect the evaporation temperature as shown in Figure 7-(c), which in turn affects the latent capacity of the evaporator and, therefore, the supply air RH fluctuates. It can be also seen in Figure 7-(c) that the air mass flow rate increases from 176 g/s to 185 g/s due to the increase of the air density, which is caused by the drop in temperature. Figure 7-(d) shows the inlet and outlet pressures of both the evaporator and condenser. Whenever the compressor RPM decreases, and therefore refrigerant flow rate, the pressure drops of both heat exchangers and the pressure ratio decrease. The decrease in pressure ratio and refrigerant mass flow rate causes a decrease of compressor power as shown in Figure 7-(e). During the test, the compressor power fluctuated between 0.5 kW and 2.0 kW. The refrigerant-side capacity and the air-side sensible, latent and total cooling capacities are shown in Figure 7-(f). It can be seen that whenever the RPM increases, the

Table 2. NEDC test conditions.

Ambient Temperature (°C)	Ambient RH (%)	Degree of Soaked Temperature (K)	Evaporator Air Velocity (m/s)	Condenser Air Velocity (m/s)	Ventilation Mode
30	50	5.6	2.3	2.5	Recirculated air

capacities increase. The locations where the refrigerant-side capacity curve is discontinuous are when the superheat at evaporator outlet was lost and therefore the capacity could not be calculated. The refrigerant-side capacity is obviously more than the air-side capacity since the refrigerant-side capacity is used not only for the air cooling but also for the refrigerant redistribution and heat capacities of the evaporator material and cabin mass.

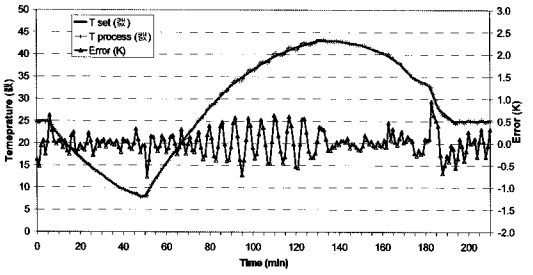

(a) Temperature

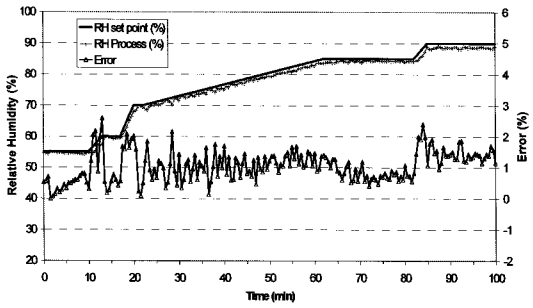

(b) Relative humidity

Fig. 5. Temperature and relative humidity control in dynamic simulator.

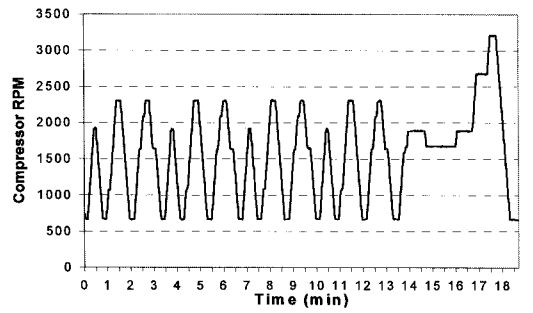

Fig. 6. Compressor RPM profile during NEDC.

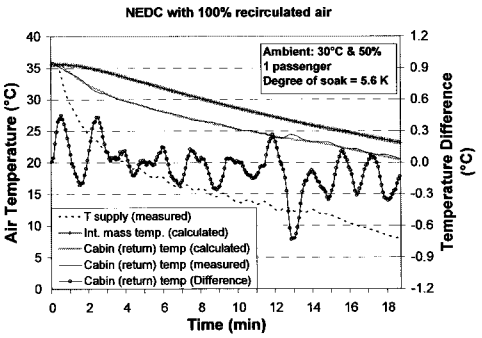

(a) Cabin air temperature

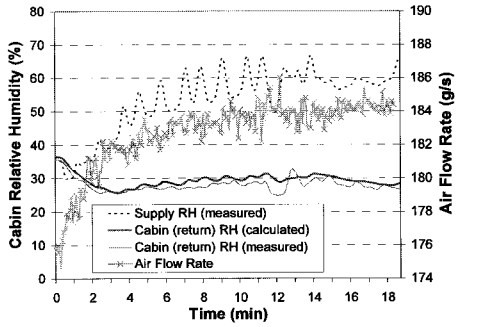

(b) Cabin relative humidity and air flow rate

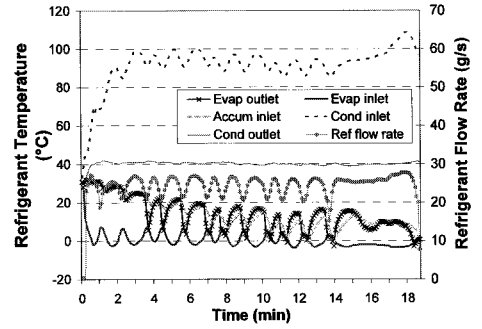

(c) Refrigerant temperatures

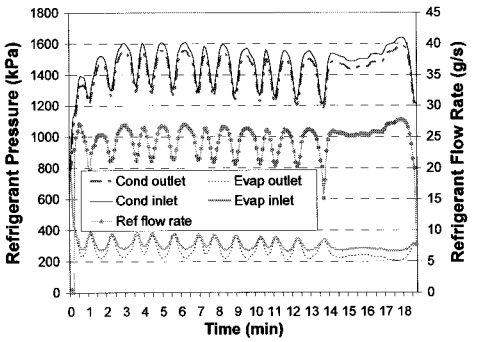

(d) Refrigerant pressures

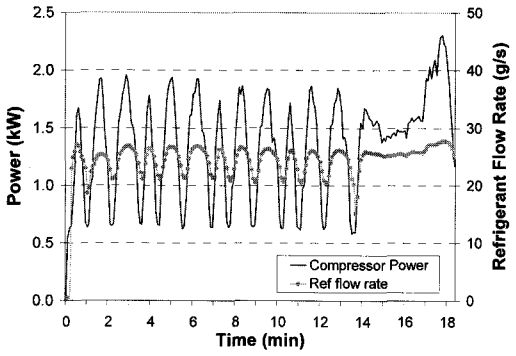

(e) Compressor power

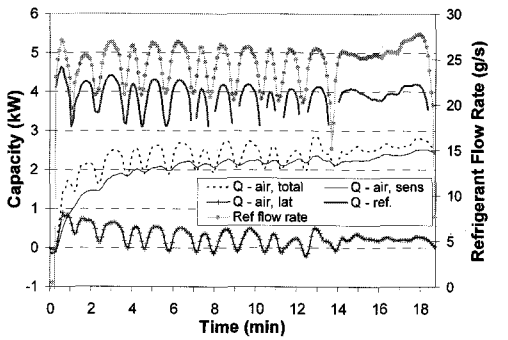

(f) Cooling capacities

Fig. 7. Tests Results during NEDC.

5. Conclusions

In this study, a novel dynamic test facility for MACs is proposed and its performance potential is demonstrated. It is a cost-effective way to run transient tests in a laboratory while eliminating the need for testing with a full-scale car in a wind tunnel. It employs a numerical cabin model whose outputs are used by the control software to dynamically adjust the air conditions inside two environmental test chambers. The cabin model takes into consideration storage and latent load terms and passengers' control settings. In this way, the AHU of the environmental chamber would have replaced the cabin loads and the conditions of the return air to the evaporator coil would have been adjusted to the return air conditions from a real car cabin. Therefore, the proposed test facility provides dynamic boundary conditions to the MAC just like the real vehicle so that the MAC behaves as if it is placed in a real vehicle. The dynamic simulator is able to impose climatic profiles such as a variation of temperature and relative humidity with respect to time and standardized drive cycles on the MAC under test. The verification tests showed that the facility was successful in controlling the temperature within a range of ± 0.7°C of the required temperature and the relative humidity within 4% of the required relative humidity. The NEDC verification test results demonstrated that detailed transient behavior of the MAC could be measured by using the dynamic simulator, which is capable of simulating real vehicle conditions. It is expected that this approach will reduce the development cost and time for evaluating the dynamic performance of the MAC. It has the potential of reproducing more realistic results than pure numerical simulations.

References

[1] Behr GmbH, 2004, www.behrgroup.com.

[2] Hill, W. et al., 2004, "Effect off windows down on vehicle fuel economy as compared to A/C load." Proceedings of SAE Alternate Refrigerant Systems Symposium, Scottsdale, Arizona.

[3] Perez, J and Rogers, P. 2003, "Crew/passneger compartment thermal load analysis using a holistic vehicle thermal model." Proceedings of SAE Vehicle Thermal Management Systems, Paper number C599/021/2003.

[4] El Bakkali, A. and Olivier, G., 2003, "Design of components libraries for the transient simulation of an automotive refrigeration loop." Proceedings of SAE Vehicle Thermal Management Systems, Paper number C599/024/2003.

[5] Kampf, H. et al., 2003, "Control technologies to optimize operating performance of R744 climate control systems." Proceedings of SAE Vehicle Thermal Management Systems, Paper number C599/052/2003.

[6] Magnetto, D. et al., 2003, "The 'cab-lounge concept' integrated systems for long-distance truck cabin thermal manegement." Proceedings of SAE Vehicle Thermal Management Systems, Paper number C599/071/2003.

[7] Hager, J., Stroh, C., and Reitbauer, R., 2003, "Optimization strategies for the transient behavior of the thermal systems of commercial vehicles." Proceedings of SAE Vehicle Thermal Management Systems, Paper number C599/019/2003.

[8] Schlenz, D. and Koch, F., 2002, "Supplimentary heater concepts to improve warm-up in vehicles with DI engines." VDA Alternate Refrigerant Winter Meeting, Saalfelden, Austria.

[9] Hrnjak, P., 2002, "Some lessons learned from SAE alternate refrigerant cooperative research program." Proceedings of SAE Alternate Refrigerant Systems Symposium, Scottsdale, Arizona.

[10] Hrnjak, P., and Hill, B., 2003, "Overview of the SAE alternate refrigerant cooperative research program." VDA Alternate Refrigerant Winter Meeting, Saalfelden, Austria.

[11] Ding, Y. and Zito, R., 2001, "Cabin heat transfer and air conditioning capacity." SAE paper number 2001-01-0284.

[12] Choquart, F. Clodic, D, El Khoury, K, Roy, D, and Petitjean, P, 2003, "Assembly model for predictive thermal comfort in vehicle." Proceedings of Vehicle Thermal Management Systems, paper number C599/005/2003.

[13] Huang, L. and Han, T., 2002, "Validation of 3-D passenger compartment hot soak and cool-down analysis for virtual thermal comfort engineering." SAE paper number 2002-01-1304.

[14] Han, T. Huang, L, Kelly, S, Huizenga, C, and Hui, Z, 2001, "Virtual thermal comfort engineering." SAE paper number 2001-01-0588.

[15] Aroussi, A. and Aghil, S., 2001, "The effects of air vents locations on the internal climate control of vehicles." SAE paper number 2001-01-0287.

[16] Khamsi, Y. and Petitjean, C., 2000, "Validation results of automotive passenger compartment and its air conditioning system modeling." SAE paper number 2000-01-0982.

[17] Thelon, W. and Zoz, S., 2003, "An approach for modeling an automotive vapor cycle refrigeration system and passenger cabin." Proceedings of Vehicle Thermal Management Systems, paper number C599/046/2003.

[18] Kohler, J. Kuhn, B, Sonnekalb, M, and Beer, H, 1996, "Numerical calculation of the distribution of temperature and heat flux in buses under the influence of the vehicle air-conditioning system." ASHRAE Transactions, pp. 432-446.

[19] Kataoka, T., 2001, "Prediction of occupant's thermal sensation under the transient environment in a vehicle compartment." SAE paper number 2001-01-0586.

[20] Roy, D. Petitjean P, Clodic, D, and El Khoury, K, 2003, "Influence of thermal preconditioning technologies on A/C system power and passengers' thermal comfort." Proceedings of Vehicle Thermal Management Systems, paper number C599/004/2003.

[21] Magna – Steyr, 2001, "KULI 5.0." by Magna Powertrain and Engineering Center Steyr GmbH & Co KG., www.magnapowertrain.com.

[22] ARMINES, 2002, "ACCSSim: Software for dynamic simulation of mobile air-conditioning systems." Centre d'Energétique, Ecole des Mines de Paris, France, www.cenerg.ensmp.fr/english/logiciel/indexACCSsim.html.

[23] Meyer, J., 2002, "HMC sonata: thermal energy efficient vehicle." SAE Automotive Alternate Refrigerant Systems Symposium.

[24] Huang, C. D., 1998, "A dynamic computer simulation model for automobile passenger compartment climate control and evaluation." Ph.D. Thesis, Michigan Technological University, USA.

[25] Rugh, J. P. Farrington, R. B., and Boettcher, J. A., 2001, "The impact of metal-free solar reflective film on vehicle climate control." SAE paper number 2001-01-1721.

[26] Kojima, K. Itoh, S, Ohtaki, H, and Watanuki, K, 1999, "An estimate of temperature in a passenger compartment by numerical simulation using the linear graph theory." SAE paper number 1999-01-1188.

[27] Wertenbach, J., 2003, Energy Analysis of Refrigerant Cycles, Automotive Alternate Refrigerant Systems Symposium.